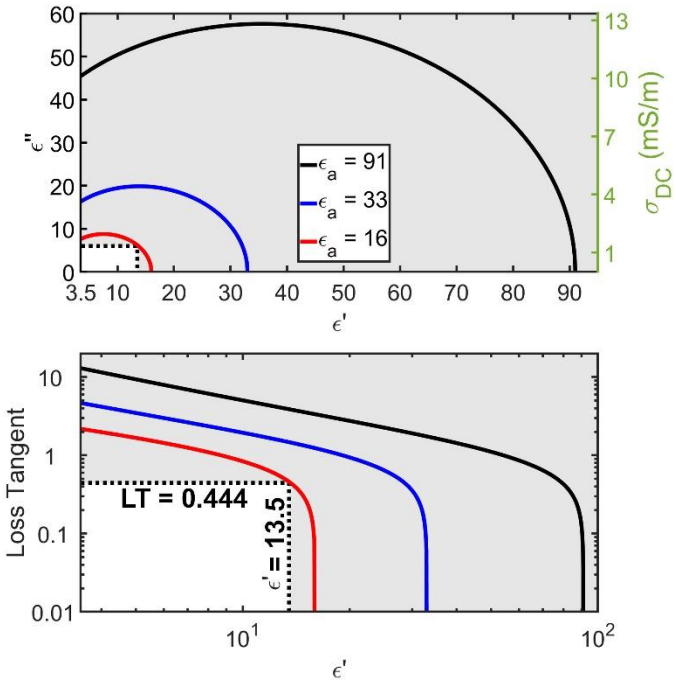

Figure 1. The solid lines display possible **(A)** ε' and ε'' and **(B)** ε' and loss tangent ($\varepsilon''/\varepsilon'$) that will combine for an ε_a equal to the 1st, 2nd (median), and 3rd quartile observed values of 16, 33, and 91, respectively. If a laboratory sample has a measured ε' and ε'' value of <13.5 and <6 (loss tangent of 0.444) at 4 MHz, respectively, then ε_a cannot obtain the 1st quartile MARSIS observed ε_a value. Note we assumed an ε' and ε'' of 3.5 and 0 for the SPLD. Additionally, the right y-axis in **(A)** shows the necessary values of σ_{DC}, if we assume all losses are conductive. Thus, σ_{DC} must be >1.3 mS m^{-1} to obtain the 1st quartile MARSIS observed ε_a value.

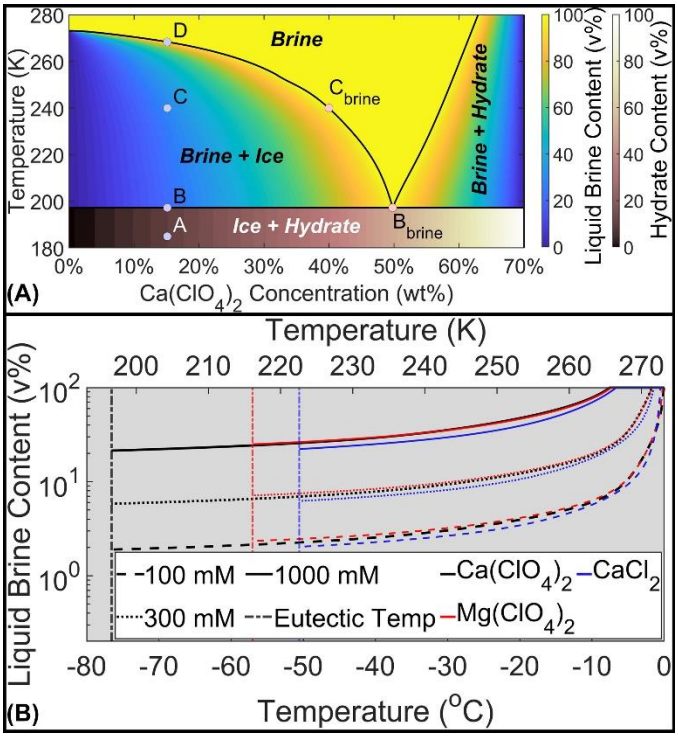

Figure 2. (A) Phase diagram of $Ca(ClO_4)_2$ with colored contours of bulk brine (parula colormap) and hydrate (pink colormap) concentrations. For example, a 700 mM (15.1 wt%) $Ca(ClO_4)_2$ sample at 185 K (Point A) has a hydrate content of ~12 vol%. At the eutectic temperature, the hydrate and ice melts to form a brine with a eutectic concentration (Point B_{brine}) and with a liquid content of ~14 vol%. At 240 K, the amount of liquid brine in the salt-H_2O mixture is ~22% (Point C), while the brine concentration is 40 wt% (Point C_{brine}). The sample then completely melts at 268.4 K (Point D). **(B)** Volume percent of brine at 100, 300, and 1000 mM versus temperature. The eutectic temperatures for $Ca(ClO_4)_2$, $Mg(ClO_4)_2$, and $CaCl_2$ are ~197.3, 216, 223 K, respectively.

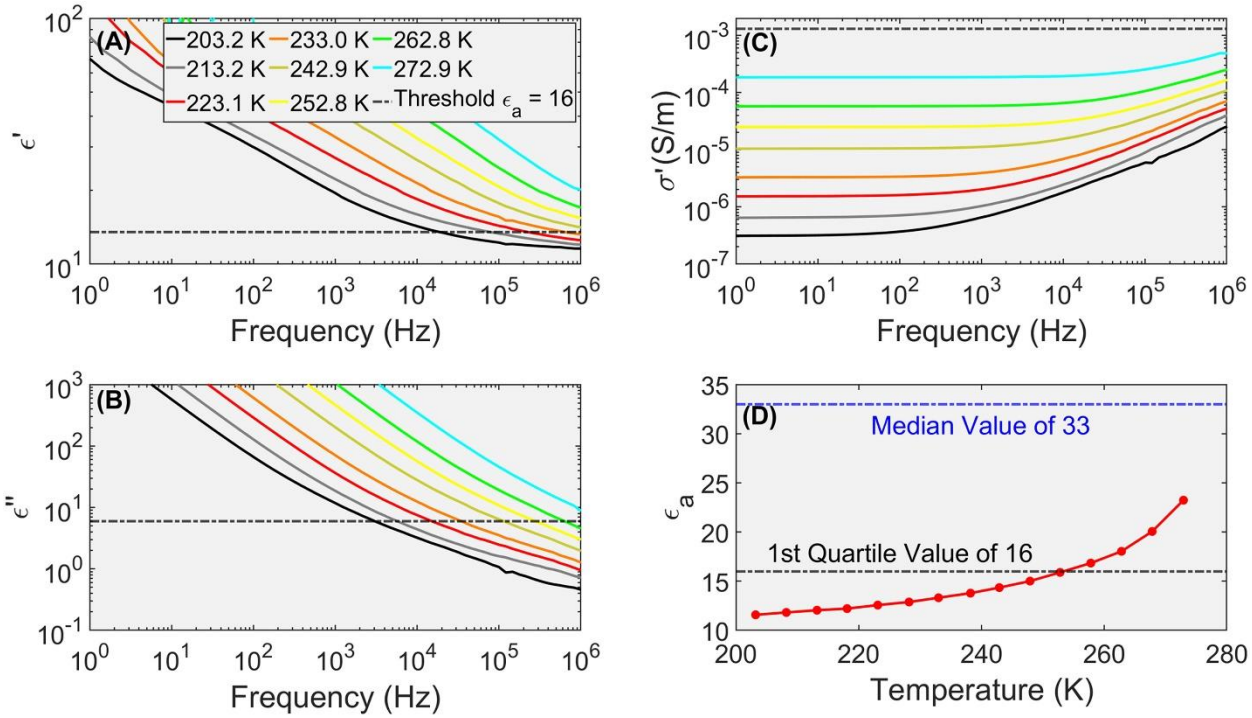

Figure 3. Real (**A**) and imaginary (**B**) part of the relative permittivity, real part of electrical conductivity (**C**) of ilmenite with 35.5% porosity. Ilmenite does have additional polarization mechanisms as well as σ_{DC} (shown by the plateau of σ′ at low frequencies). The apparent permittivity (**D**) is calculated assuming an SPLD with $\varepsilon' = 3.5$ as a function of temperature. This shows that the polarizations and σ_{DC} are not large enough to produce ε_a values within the observed range at temperatures below ~252.8 K.

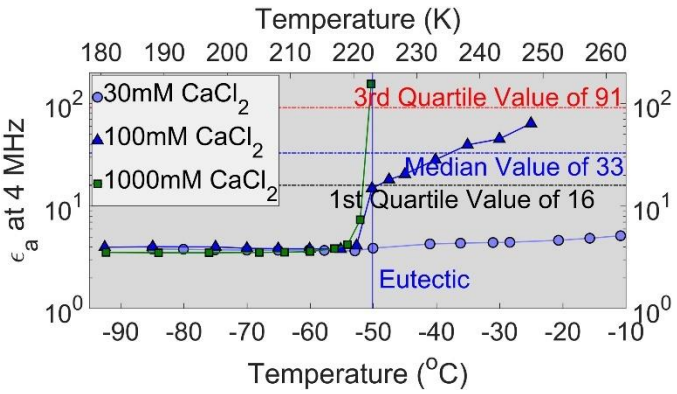

Figure 4. Apparent permittivity of various concentrations of $CaCl_2$ as a function of temperature. Of these concentrations, 100 mM (1.1 wt%) $CaCl_2$ is near the 1st quartile value of the observed MARSIS ε_a at 233 K.

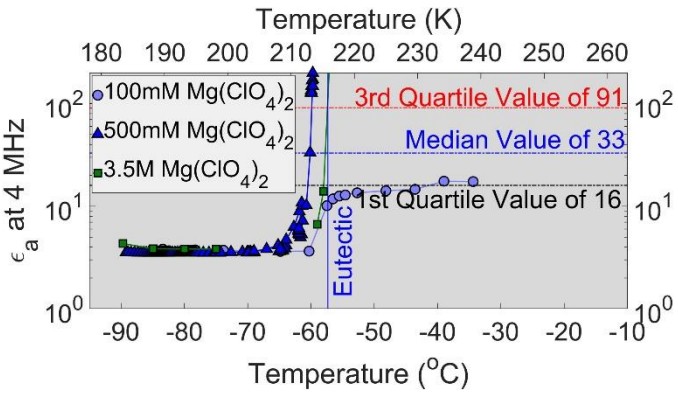

Figure 5. Apparent permittivity of various concentrations of $Mg(ClO_4)_2$ as a function of temperature. Of these concentrations, 100 mM (2.2 wt%) $Mg(ClO_4)_2$ is not able to obtain the 1st quartile value of the observed MARSIS ε_a at 216 K, while 500 mM (10 wt%) and 3.5 M (44 wt%) $Mg(ClO_4)_2$ possesses an ε_a that are larger than the 3rd quartile value above the eutectic temperature.

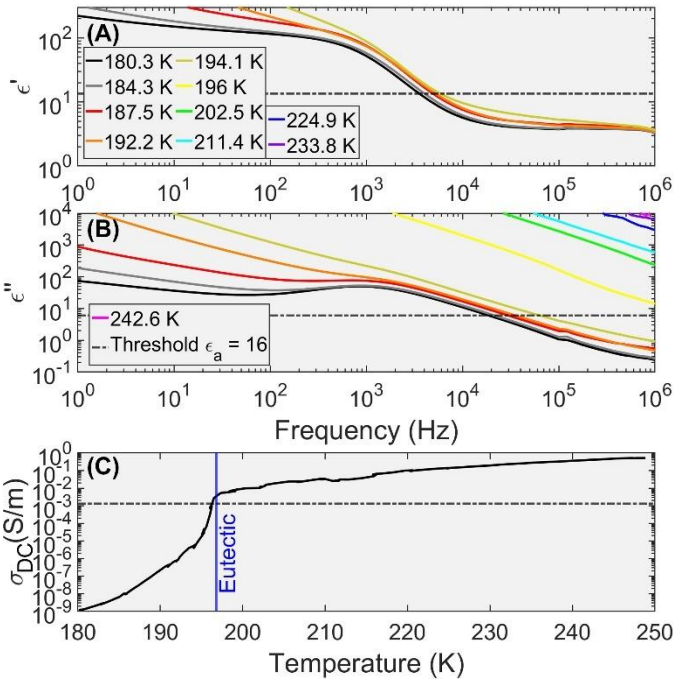

Figure 6. Real (**A**) and imaginary (**B**) part of the relative permittivity, and modeled DC conductivity (**C**) of 300 mM (6.9 wt%) $Ca(ClO_4)_2$ as a function of temperature. (**A** and **B**) show spectrum at selected temperatures, while (**C**) shows all the spectrum fitted over the entire measurement run. Note below the eutectic temperature the sample shows a dielectric relaxation of ice, however once the eutectic is reached the sample becomes conductive and ε' is not shown as it has little accuracy as all the energy is being dissipated conductively.

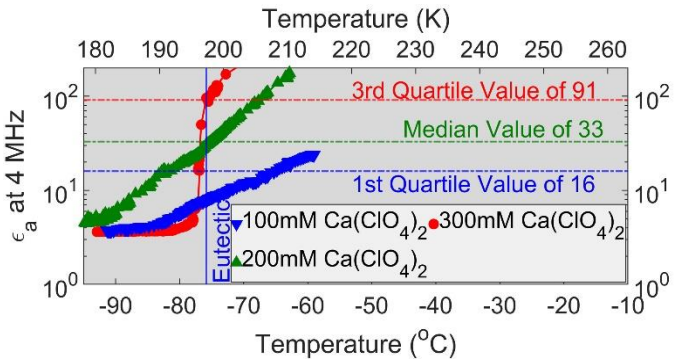

Figure 7. Apparent permittivity of mixtures as a function of temperature. The 200 mM (4.7 wt%) and 300 mM (6.9 wt%) $Ca(ClO_4)_2$ samples are near the observed median and 3rd quartile value at temperatures greater than the eutectic, respectively. The 100 mM (2.4 wt%) $Ca(ClO_4)_2$ sample is below the 1st quartile value. Note the 100 and 200 mM samples never froze, thus the values below the eutectic temperature are for a metastable brine.

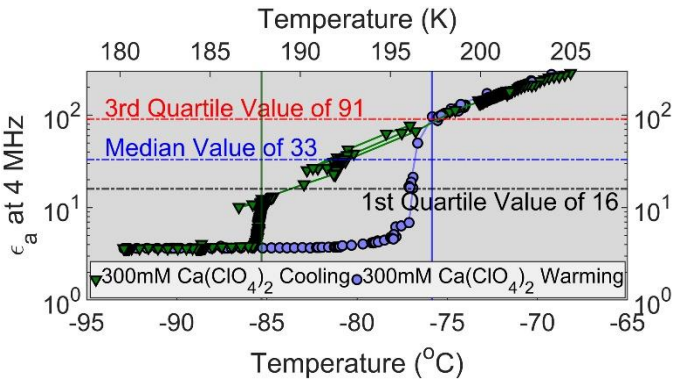

Figure 8. Apparent permittivity of 300 mM (6.9 wt%) $Ca(ClO_4)_2$ as a function of temperature for cooling and warming measurements. Note that the ε_a continues it constant decrease with temperature as it is cooled below the eutectic temperature, the brines in this sample then froze at a temperature of 187.9 K (vertical green line). Upon warming the brines then fully thaw at the eutectic temperature of 197.3 K (vertical blue line) and reach the same ε_a as during cooling.

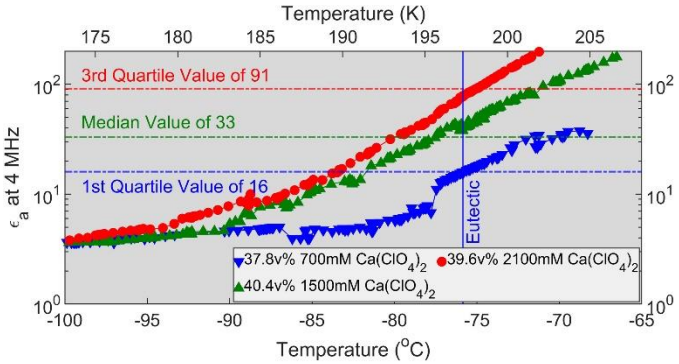

Figure 9. Fine-grained sand mixed with salt-H_2O mixtures of $Ca(ClO_4)_2$. Samples of 700 mM (15.1 wt%), 1.5 M (29.1 wt%), and 2.1 M (38.1 wt%) $Ca(ClO_4)_2$ are near the 1st quartile, median, and 3rd quartile values of ε_a, respectively, at the eutectic temperature of $Ca(ClO_4)_2$. Note that the displayed data do not possess the eutectic temperature jump indicative of melting. Thus, indicating that the $Ca(ClO_4)_2$ never froze even when lowered to below 173 K. Warming cycles (shown) and the cooling cycle (not shown for simplicity) show no hysteresis, further suggesting the brine is metastable below the eutectic temperature.

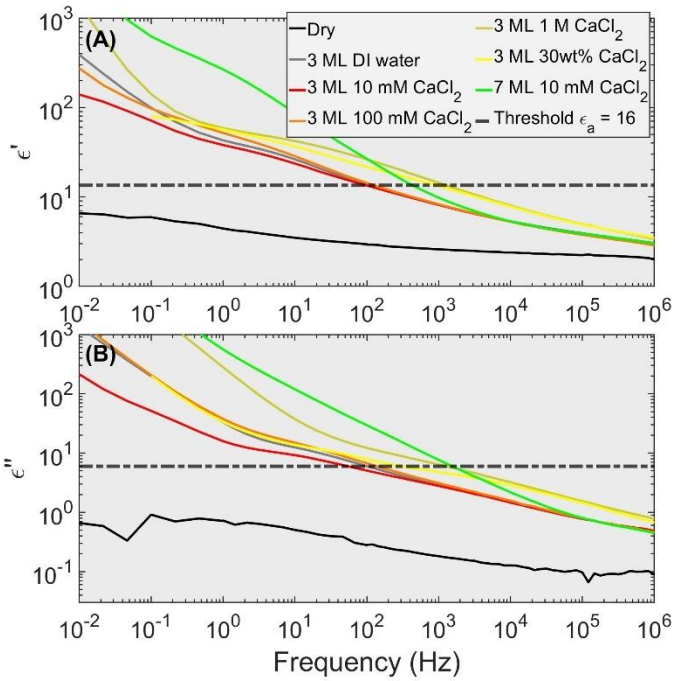

Figure 10. Compilation of ε' (**A**) and ε'' (**B**) values of dry and low-saturation measurements of Texas Calcium Montmorillonite (STx-1) at ~193.2±0.2 K, where ML is the number of calculated monolayers. At this temperature, the samples show no enhanced ε' or ε'' that could explain the MARSIS observed values measurements.

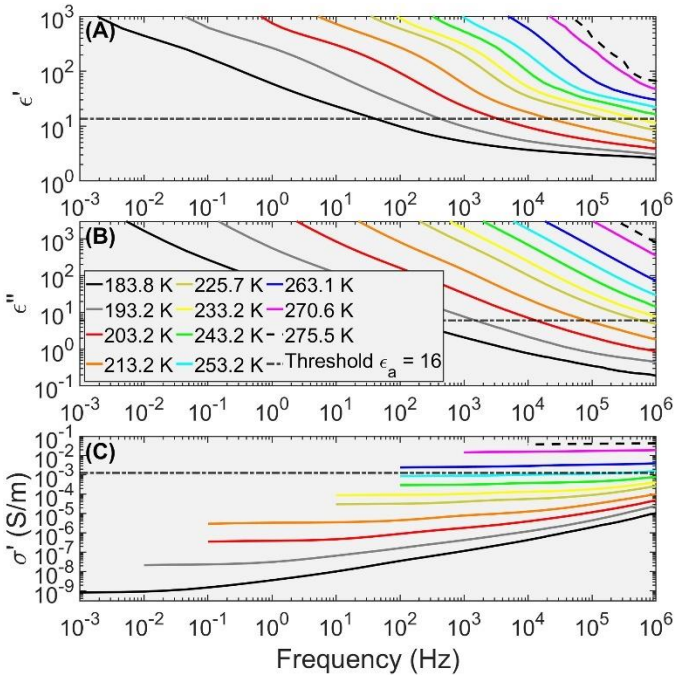

Figure 11. STx-1 measurements with 7 ML 100 mM (1.1 wt%) $CaCl_2$ for ε' (**A**), ε'' (**B**), and σ' (**C**). This sample had a STx-1, 100 mM $CaCl_2$, and air mass (volume) concentration of 70.4 mass% (28.0 vol%), 29.6 mass% (32.4 vol%), and 0 mass% (39.6 vol%), respectively. At 1 MHz, the electrical properties cannot obtain the ε_a threshold when temperatures are <233 K.

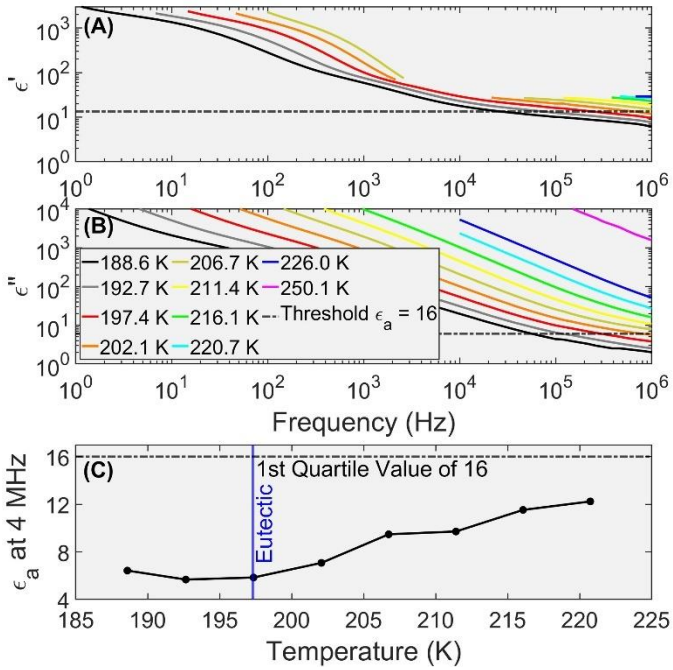

Figure 12. Complex electrical property measurements SAz-1 saturated with 500 mM (11.2 wt%) $Ca(ClO_4)_2$ with a mass (volume) concentration of 45.8 mass% (25.5 vol%) sand and 54.2 mass% (74.5 vol%) of salt-H_2O. (**A**) ε', (**B**) ε'', and (**C**) ε_a of the mixture shows that the sample has low-frequency broad dielectric relaxations and high DC conductivity, but never approaches the observed 1st quartile value.

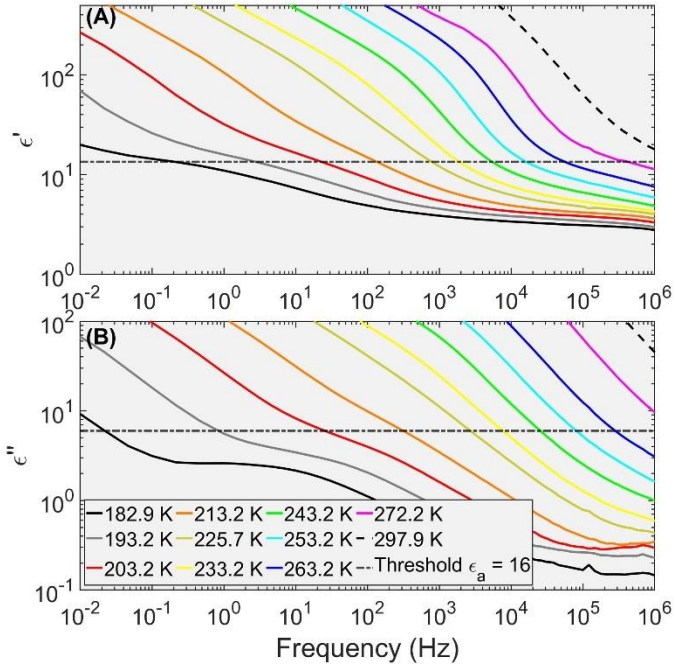

Figure 13. Complex electrical property measurements of JSC Mars-1 with 7 ML of 100 mM (1.1 wt%) $CaCl_2$. JSC Mars-1, 100 mM $CaCl_2$, and air in this partially-saturated sample had a mass (volume) concentration of 82.2 mass% (43.3 vol%), 17.8 mass% (17.9 vol%), and 0 mass% (38.8 vol%), respectively. The electrical properties do not approach the ε_a threshold for the 1st quartile value until the sample becomes completely unfrozen (>273 K). Thus, even with multiple polarization mechanisms of adsorbed water and ice combined with DC conductivity cannot approach the observed MARSIS threshold.

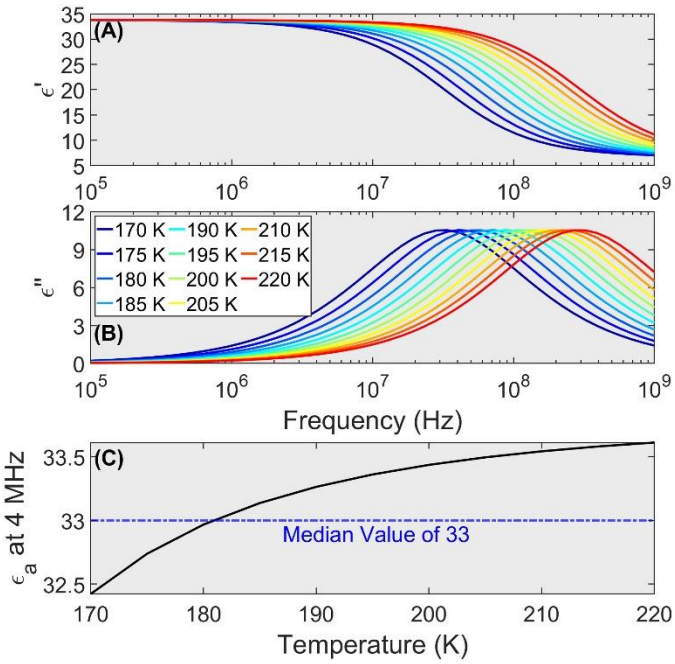

Figure 14. Electrical properties of grey hematite based on radar measurements modeled by *Stillman and Olhoeft* (2008). Note this model represent the measured sample that had a porosity of 41% and a grey hematite volume concentration of 59%. This high-frequency relaxation does not greatly affect ε_a at 4 MHz over typical SPLD temperatures.

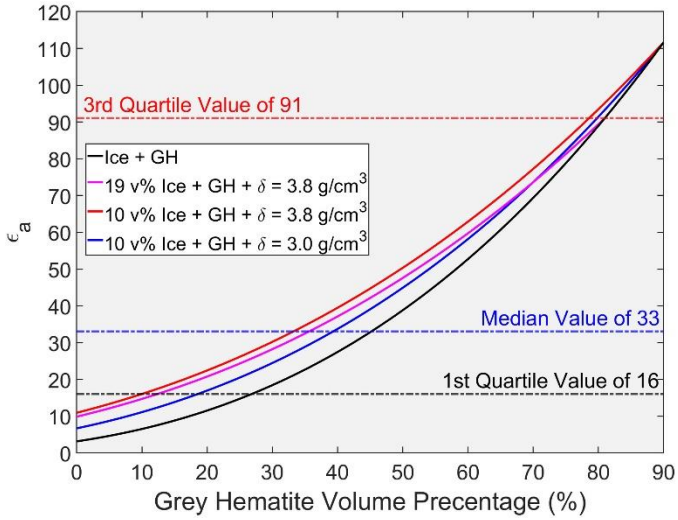

Figure 15. Four grey hematite (GH) mixing models are used to estimate the concentrations of ice, GH at 200 K, ultramafic (density δ = 3.8 g cm^{-3}) and mafic (δ = 3.0 g cm^{-3}) grains that would match the observed MARSIS ε_a values. Precise values are given in **Table 1**.

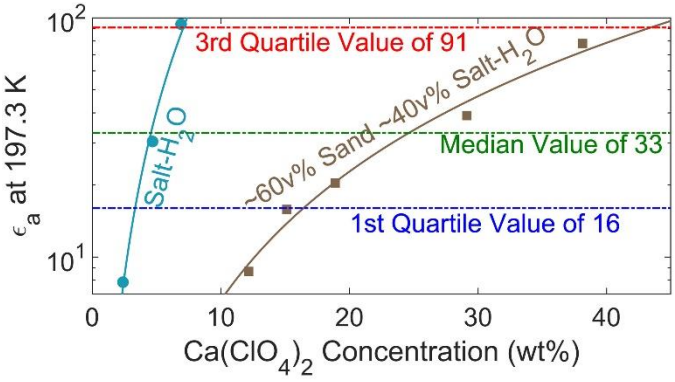

Figure 16. Apparent permittivity at the eutectic temperature versus calcium perchlorate mass concentration. The three experiments (symbols) of the salt-H_2O mixtures were fit (solid line) with a power law to calculate the 1st quartile, median, and 3rd quartile values of 3.3, 4.6, and 7.1 wt%, respectively. The five experiments of the sand mixtures with salt-H_2O were similarly fit with a power law to calculate the 1st quartile, median, and 3rd quartile values of 16.4, 24.6, and 43.4 wt%, respectively.

Table 1. Values of the four grey hematite (GH) mixing models shown in **Figure 15** at the observed 1st and 3rd quartile and median values of ε_a. The grain density δ_G values of 3.8 and 3.0 g cm^{-3} were used to represent an ultramafic and mafic grain density, respectively, and converted to permittivity using Eq 1. A δ_G of 5.26 and 0.917 g cm^{-3} were used for GH and ice, respectively, to calculate the bulk density δ_B. Note we assume that all pore space is filled by ice as ground ice should be stable under the SPLD. We also calculate δ_B by neglecting the contribution of ice to allow us to compare to terrestrial δ_B of rocks. In the comment's column, we assume that any rocks with a δ_B larger than 3.5 g cm^{-3} are too high (the largest density of the volcanic samples measured by *Rust et al.* (1999) and *Schmulevich et al.* (1971) was a gabbro at 3.39 g cm^{-3}). Additionally, we commented that any solution with a GH concentration greater than 30 vol% was too large as TES spectroscopic observations detected a maximum of 15 vol% of GH over Aram Chaos and Meridiani Planum (*Glotch and Christensen*, 2005).

ε_a	Ice	GH	δ_G = 3.8 g cm^{-3}	δ_G = 3.0 g cm^{-3}	δ_B g cm^{-3}	δ_B g cm^{-3} when replace ice with air	Comments
91	19.0%	81.0%			4.43	4.26	High density; Significant vol% of GH
33	54.8%	45.2%			2.87	2.37	Significant vol% of GH
16	73.2%	26.8%			2.08	1.41	Possible
91	19.0%	81.0%	0.0%		4.43	4.26	High density; Significant vol% of GH
33	19.0%	35.6%	45.4%		3.77	3.60	High density; Significant vol% of GH
16	19.0%	12.4%	68.6%		3.43	3.26	Possible
91	10.0%	78.6%	11.4%		4.66	4.57	High density; Significant vol% of GH
33	10.0%	33.2%	56.8%		4.00	3.90	High density; Significant vol% of GH
16	10.0%	10.0%	80.0%		3.66	3.57	High density
91	10.0%	79.8%		10.2%	4.59	4.50	High density; Significant vol% of GH
33	10.0%	39.2%		50.8%	3.68	3.59	High density; Significant vol% of GH
16	10.0%	18.5%		71.5%	3.21	3.12	Possible